

Constraint on the potassium content for the superconductivity of potassium-intercalated phenanthrene

Qiao-Wei Huang,^{1,2} Guo-Hua Zhong,³ Jiang Zhang,² Xiao-Miao Zhao,^{1,2} Chao Zhang,^{4,5} Hai-Qing Lin,^{3,5} and Xiao-Jia Chen^{1,6,a)}

¹Center for High Pressure Science and Technology Advanced Research, Shanghai 201203, China

²Department of Physics, South China University of Technology, Guangzhou 510640, China

³Center for Photovoltaics and Solar Energy, Shenzhen Institutes of Advanced Technology, Chinese Academy of Sciences, Shenzhen 518055, China

⁴Department of Physics, Yantai University, Yantai 264005, China

⁵Beijing Computational Science Research Center, Beijing 100084, China

⁶Geophysical Laboratory, Carnegie Institution of Washington, Washington DC 20015, USA

(Received 26 November 2013; accepted 25 February 2014; published online 17 March 2014)

Raman-scattering measurements were performed on K_x phenanthrene ($0 \leq x \leq 6.0$) at room temperature. Three phases ($x = 3.0, 3.5,$ and 4.0) are identified based on the obtained Raman spectra. Only the K_3 phenanthrene phase is found to exhibit the superconducting transition at 5 K. The C–C stretching modes are observed to broaden and become disordered in K_x phenanthrene with $x = 2.0, 2.5, 6.0$, indicating some molecular disorder in the metal intercalation process. This disorder is expected to influence the nonmetallic nature of these materials. The absence of metallic character in these nonsuperconducting phases is found from the calculated electronic structures based on the local density approximation. © 2014 AIP Publishing LLC. [<http://dx.doi.org/10.1063/1.4868437>]

I. INTRODUCTION

Recently, polyaromatic hydrocarbons (PAHs) have attracted considerable interest because of the discovery of superconductivity in hydrocarbon systems. The PAH compounds, such as phenanthrene¹ ($C_{14}H_{10}$), picene² ($C_{22}H_{14}$), coronene³ ($C_{24}H_{12}$), and 1,2:8,9-dibenzopentacene⁴ ($C_{30}H_{18}$), are found to exhibit superconductivity by doping with alkali or alkali-earth metal atoms. Other organic superconductors have also been reported, such as tetrathiafulvalene (TTF),⁵ bis-ethylenedithio-TTF (BEDT-TTF, abbreviated as ET),⁶ and tetramethyltetraselenafulvalene (TMTSF)⁷ derivatives. Hydrocarbon superconductors are novel superconducting systems with intriguing properties. Consequently, much effort has been devoted to investigate their physical properties to search for new hydrocarbon superconductors with high superconducting transition temperatures (T_c) and to understand the mechanism of superconductivity. Based on previous findings, the T_c of hydrocarbon superconductors is found to substantially increase with increasing number of benzene rings,^{1–4} and it reaches 33.1 K in K-doped 1,2:8,9-dibenzopentacene⁴ (the highest T_c in organic superconductors). The feature of “armchair” edge type, which is regarded as a fundamental factor for the superconductivity of hydrocarbon system, is common in hydrocarbon superconductors, whereas “zigzag” edge type is not common.^{1,2,4,8} Furthermore, hydrocarbon superconductors are a low-dimensional system with strong electron–phonon and electron–electron interactions, which both may be involved in superconductivity, as suggested by theoretical studies.^{9–13}

The mechanism of superconductivity in PAHs is still not completely understood owing to the complexity of hydrocarbon systems. However, many theoretical studies have thoroughly described the mechanism of superconductivity.^{14–16} Rigid band approximation calculations on $K_{3,0}$ picene show that the electrons transferred to organic molecules from intercalated potassium atoms occupy its lowest unoccupied molecular orbital, leading to a metallic state. However, this approximation does not consider the influence of the electron–intramolecular-vibration interaction in K-doped picene, and the electron–phonon interaction is experimentally observed by photoemission spectroscopy.¹⁷ Therefore, charge transferred from the intercalated potassium atoms is expected to play an important role in the superconductivity of PAHs. Therefore, the importance of the electron–intramolecular-vibration interaction cannot be ignored in the investigation of the superconducting properties of this family.

Phenanthrene is the simplest molecule with three benzene rings that exhibits an armchair configuration. Cation-doped phenanthrene has a larger superconducting volume fraction than other PAH-based superconductors.^{1–4} The relationship between cation doping and superconductivity has not yet been established. It remains unclear whether adding more of the cation element increases the superconductivity in this material. Raman scattering is a powerful technique to study the vibrational properties of aromatic hydrocarbon molecules^{18–21} and their doped derivative compounds.^{1–4} This technique has proven to be very powerful in the determination of the x value in A_xC_{60} and A_x picene.^{22–24} Raman scattering directly probes the number of electrons transferred to the molecule based on the shifts of the Raman modes.

In this study, we report a detailed Raman scattering study of K_x phenanthrene ($0 \leq x \leq 6$) at room temperature. We

^{a)}Electronic mail: xjchen@ciw.edu

determine the number of electrons transferred to the phenanthrene molecule. Our results suggest the phase separation and intermediate phase in the range $x = 0$ – 6.0 . Combined with density functional calculations, we obtain an experimental constraint on the superconductivity of potassium-intercalated phenanthrene.

II. EXPERIMENTAL DETAILS

Phenanthrene (98% purity, colorless crystals) was purchased from Alfa Aesar and used without further purification. For each composition, phenanthrene powder was mixed with potassium in a glass tube, and the glass tube was sealed at 10^{-4} par. Then, the sample was heated to about 470 K for 40 h. After the annealing process, the sample changed to a uniform black color. Magnetic susceptibility and Raman spectroscopy were performed on the synthesized samples without any exposure to air. The magnetization M was measured with a SQUID magnetometer (Quantum Design) at an applied field H of 10 Oe in a temperature range from 2.5 to 8 K. Raman spectra were measured in backscattering geometry with visible laser excitation (633 nm) and power less than 5 mW at room temperature. All the samples were sealed in capillaries without exposure to air.

III. RESULTS AND DISCUSSION

Raman spectra of K_x phenanthrene are shown in Fig. 1 for different x values. The spectrum of pristine phenanthrene agrees well with previous works.²⁵ There are four intense Raman peaks (409, 829, 1036, and 1350 cm^{-1} for pristine phenanthrene) that can be used to compare pristine and doped phenanthrene. As shown in Fig. 1, the Raman peaks of K_x phenanthrene shift to lower frequencies compared with pristine phenanthrene, which indicates the mode softening effect from alkali-metal doping. The doping-induced downshift is reasonably common in the intercalation compounds of carbon-based and hydrocarbon materials, such as doped graphite, doped carbon nanotubes, A_xC_{60} ($A = K, Rb$), and K_x picene.^{22–24,26,27} These downshifts provide evidence of charge transfer between the dopants and the phenanthrene molecules, and can be explained by the elongation of the intralayer C–C bond length because of the intercalation of alkali metal into the solids.

In Fig. 2, the experimental frequencies of the Raman peak located at 1350 cm^{-1} for pristine phenanthrene are plotted as a function of x for K_x phenanthrene. In the case of K_x picene,²⁴ the number of transferred electrons and three stoichiometries were identified by the Raman measurement: K_2 picene, $K_{2.5}$ picene, and K_3 picene. Consequently, we used Raman spectroscopy to determine the actual number of electrons transferred from the dopants in K_x phenanthrene. As shown in Fig. 2, the Raman peak located at 1350 cm^{-1} for pristine phenanthrene is approximately located at three discrete values for x in the range 0 to 6.0: 1322 , 1325 , and 1328 cm^{-1} . We also found that different discrete values of the Raman peaks are observed in samples with the same value of x , as shown in Fig. 2. Thus, the actual number of electrons

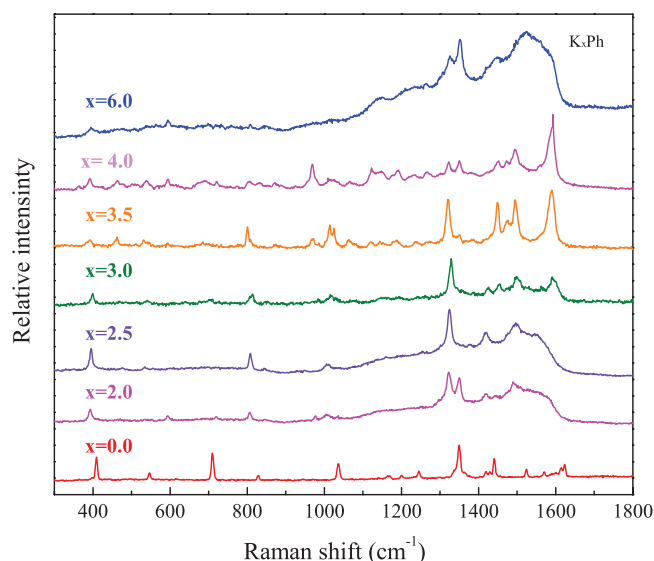


FIG. 1. Room temperature Raman spectra of K_x phenanthrene ($0 \leq x \leq 6$).

transferred to the phenanthrene molecules is not related to the value of x .

In our experiments, the sample with the Raman peak located at 1328 cm^{-1} shows superconductivity at 5 K, as shown in Fig. 3. Donation of three electrons to an aromatic hydrocarbon molecule is regarded as a fundamental factor for superconductivity.^{1–4} Consequently, we expect that three electrons are transferred to the phenanthrene molecule in the superconducting phase. As there is a 22 cm^{-1} downshift for the 1350 cm^{-1} mode in $K_{3.0}$ phenanthrene, each electron contributes a 7 cm^{-1} redshift to the Raman mode at 1350 cm^{-1} . Based on the Raman shift, there are two phases in K_x phenanthrene: $K_{3.0}$ phenanthrene (1328 cm^{-1}) and $K_{4.0}$ phenanthrene (1322 cm^{-1}). Furthermore, we observed the frequency 1325 cm^{-1} , which is intermediate between 1328 and 1322 cm^{-1} and suggests the existence of the $K_{3.5}$ phenanthrene phase. Similar to the case of K_x picene, only three discrete phases can be produced in K_x phenanthrene,

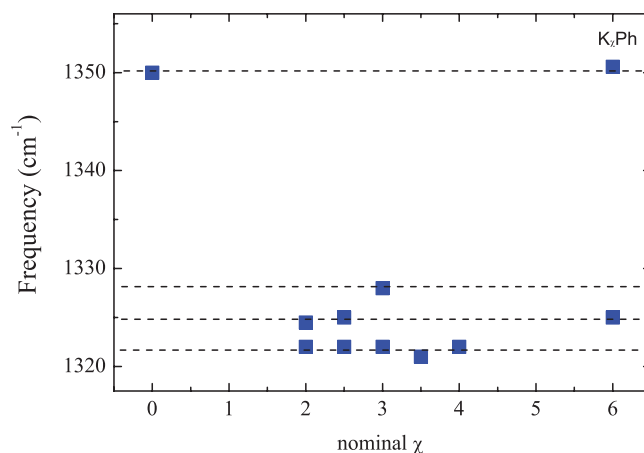


FIG. 2. Dependence of the frequency of the experimental Raman peak at 1350 cm^{-1} for pristine phenanthrene on the value of x in K_x phenanthrene ($0 \leq x \leq 6$).

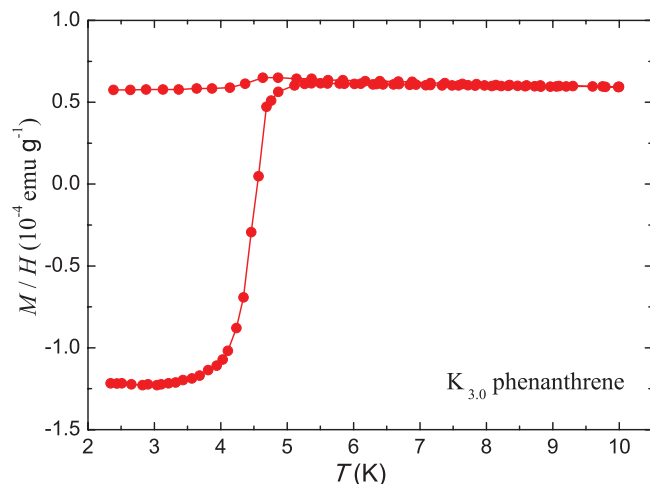


FIG. 3. Temperature dependence of M/H for $K_{3.0}$ phenanthrene showing the superconducting transition at 5 K in the zero-field cooling and field cooling measurements at applied magnetic field of 10 Oe.

which are independent of the value of x , and other phases with different composition of potassium cannot be formed.

Among the three possible phases, only the $K_{3.0}$ phenanthrene phase shows the superconducting transition based on the magnetization measurements. This observation is consistent with the previous discovery of superconductivity¹ in phenanthrene, which reported that only the sample with composition $K_{3.0}$ phenanthrene shows superconductivity in a series of K_x phenanthrene samples with different potassium contents and all other samples do not show any features of superconductivity. However, our results suggest that the actual number of electrons transferred to the phenanthrene molecules is not related to the value of x . The superconductivity of K_x phenanthrene can only be obtained when the actual number of electrons transferred to the molecule is equal to three. Consequently, the donation of three electrons to a molecule plays an important role on the superconductivity, and is independent of the donation of the alkali metal.

Based on the analysis of the positions of the Raman modes, there are three phases in K_x phenanthrene. For all of the samples, we only observed superconductivity in the phase with $x = 3.0$. The samples with other phases did not show any features of superconductivity. Additionally, the phases of $K_{3.5}$ phenanthrene and $K_{4.0}$ phenanthrene are much more stable than the superconducting phase ($K_{3.0}$ phenanthrene). These two nonsuperconducting phases can easily be obtained for any x value; thus, the superconductivity is dependent on the number of electrons transferred to the aromatic molecule, and is also very sensitive to the external conditions, especially the annealing conditions.

To investigate the stability of the superconducting $K_{3.0}$ phenanthrene sample, we examined the Raman-active modes of $K_{3.0}$ phenanthrene after a further annealing process (Fig. 4). The blue line shows the Raman spectrum of $K_{3.0}$ phenanthrene, which shows the superconducting transition at 5 K, annealed at 473 K for 40 h (initial annealing

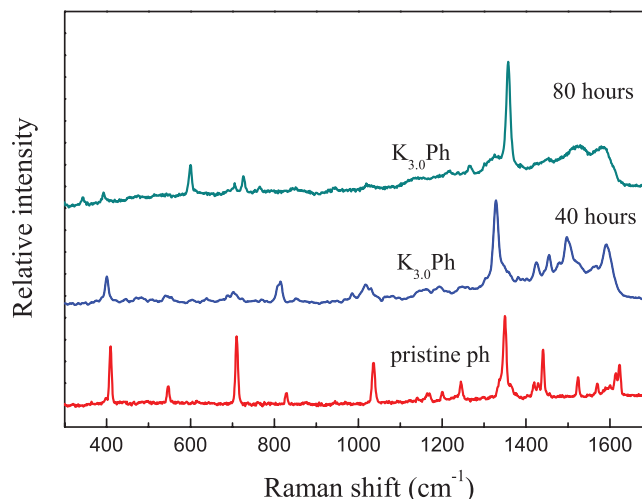


FIG. 4. Raman spectra of $K_{3.0}$ phenanthrene annealed at different times compared with pristine phenanthrene.

process). In addition, we performed another annealing process at 453 K for 40 h after the initial preparation, giving a total annealing time of 80 h. Based on the magnetization measurement, the superconductivity of $K_{3.0}$ phenanthrene disappears after the second annealing process. After the initial annealing process (473 K for 40 h), most of the Raman modes shift to lower frequencies owing to the intercalation of potassium atoms. After the further annealing process (453 K for 40 h), however, some Raman modes are different to those in $K_{3.0}$ phenanthrene. The vibration modes at 409, 710, 1036, 1350 cm^{-1} for $K_{3.0}$ phenanthrene remain but are weaker, and some new peaks are present in the Raman spectrum. A Raman spectrum consistent with $K_{3.0}$ phenanthrene is still observed with the shorter annealing time, where the peak at 1350 cm^{-1} for pristine phenanthrene shifts to the lower frequency of 1328 cm^{-1} . On the other hand, the corresponding peak of $K_{3.0}$ phenanthrene prepared by a longer annealing time shifts to a frequency of 1357 cm^{-1} , indicating that less electrons are transferred to the phenanthrene molecule from the potassium atoms. As well as the Raman modes originating from the phenanthrene molecule, new peaks are observed at 360, 720, and 1270 cm^{-1} in the sample prepared with longer annealing time, suggesting that a different molecular arrangement or a new material are produced in the further annealing process.

The vibration modes in the frequency range from 1500 to 1700 cm^{-1} represent the C–C stretching modes. In the Raman spectra of K_x phenanthrene ($x = 2.0, 2.5, \text{ and } 6.0$), most of the Raman peaks corresponding to the C–C stretching modes are absent or featureless. This is possibly related to molecular distortion of the benzene rings and slight molecular arrangement owing to the doping of potassium metal. This indicates that the rigid-band approximation is not valid in the calculations of hydrocarbons. By doping potassium metal and using density functional theory calculations, we have theoretically investigated the crystal and electronic structures of solid K_x phenanthrene. The calculations were performed using the Vienna *ab initio* simulation package (VASP)²⁸ based on the

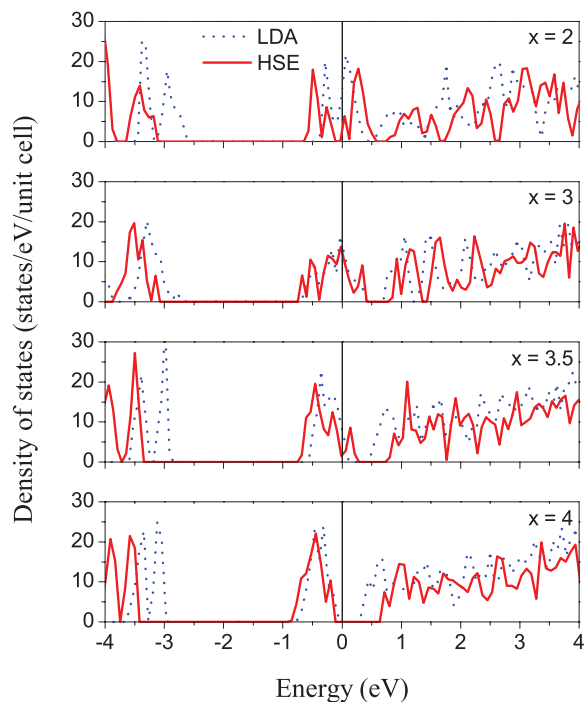


FIG. 5. Calculated density of states of K_x phenanthrene for $x = 2, 3, 3.5,$ and 4 . Dotted and solid lines are the LDA and HSE results, respectively.

local density approximation (LDA).²⁹ Considering the effects of electronic correlation in potassium-doped PAHs,^{12,30} the hybrid functional method (HSE)^{31–33} was used to overcome the limitations of the LDA. Figure 5 shows the calculated density of states for four selected doping concentrations. From the results based on LDA (dotted lines), solid K_x phenanthrene exhibits metallic character at $x = 2, 3,$ and 3.5 while it is an insulator at $x = 4$. Noticeably, the density of states at the Fermi level for $x = 2$ and $x = 3.5$ are visibly less than for $x = 3$, which indicates that there is a decrease of the superconducting electronic states when x deviates from 3. In fact, under the effect of electronic correlation, the Fermi level is located in the pseudo-gap of the electronic states of K_2 phenanthrene and $K_{3.5}$ phenanthrene systems, as shown HSE results (solid lines) in Fig. 5. Consequently, the metallic feature is absent in the systems where deviating from $x = 3$, which also explains the absence of superconductivity in these materials.

In addition, we also found that the arrangement of the phenanthrene molecule and the K atomic positions will result in variations of the density of states at the Fermi level. This indirectly indicates that the superconductivity in K_x phenanthrene depends not only on the doping content of the alkali metal but also on the molecular arrangement and the atomic position of the alkali metal. However, the location of the potassium atom is still unclear and future structural determination, especially from neutron diffraction, is required to further explore the mechanisms of superconductivity. However, the doping constraint on the superconductivity discovered here is important for understanding the mechanism of superconductivity at least in phenanthrene-based superconductors.

IV. CONCLUSIONS

In summary, we have performed Raman scattering measurements on K_x phenanthrene to identify the doping–superconductivity phase relationship. We found that three phases exist in K-doped phenanthrene with $x = 3, 3.5,$ and 4 . Only the $x = 3$ phase was found to exhibit superconductivity at $T_c = 5$ K. Consequently, the donation of three electrons to a molecule is essential for superconductivity, and is independent of the donation of the alkali metal. This experimental finding of the cation constraint on superconductivity will be helpful for designing or synthesizing new hydrocarbon superconductors with high transition temperatures.

ACKNOWLEDGMENTS

We would like to express our appreciation to Professor Xian-Hui Chen at the University of Science and Technology of China for his hospitality to allow us to use his laboratory in sample synthesis. This work was supported in part by EFree, an Energy Frontier Research Center funded by the U.S. Department of Energy (DOE), Office of Science under DE-SC0001057. The work done in China was supported by the Cultivation Fund of the Key Scientific and Technical Innovation Project Ministry of Education of China (Project No. 708070), the Shenzhen Basic Research Grant (Grant No. JC201105190880A), the National Natural Science Foundation of China (No. 11274335), and the Fundamental Research Funds for the Central Universities SCUT (No. 2014ZZ0069).

- ¹X. F. Wang, R. H. Liu, Z. Gui, Y. L. Xie, Y. J. Yan, J. J. Ying, X. G. Luo, and X. H. Chen, *Nat. Commun.* **2**, 507 (2011).
- ²R. Mitsuhashi, Y. Suzuki, Y. Yamanari, H. Mitamura, T. Kambe, N. Ikeda, H. Okamoto, A. Fujiwara, M. Yamaji, N. Kawasaki, Y. Maniwa, and Y. Kubozono, *Nature* **464**, 76 (2010).
- ³Y. Kubozono, H. Mitamura, X. Lee, X. He, Y. Yamanari, Y. Takahashi, Y. Suzuki, Y. Kaji, R. Eguchi, K. Akaike, T. Kambe, H. Okamoto, A. Fujiwara, T. Kato, T. Kosugi, and H. Aoki, *Phys. Chem. Chem. Phys.* **13**, 16476 (2011).
- ⁴M. Xue, T. Cao, D. Wang, Y. Wu, H. Yang, X. Dong, J. He, F. Li, and G. F. Chen, *Sci. Rep.* **2**, 389 (2012).
- ⁵A. M. Kini, U. Geiser, H. H. Wang, K. D. Carlson, J. M. Williams, W. K. Kwok, K. G. Vandervoort, J. E. Thompson, and D. L. Stupka, *Inorg. Chem.* **29**, 2555 (1990).
- ⁶H. Taniguchi, M. Miyashita, K. Uchiyama, K. Satoh, N. Mori, H. Okamoto, K. Miyagawa, K. Kanoda, M. Hedo, and Y. Uwatoko, *J. Phys. Soc. Jpn.* **72**, 468 (2003).
- ⁷D. Jerome, A. Mazaud, M. Hirano, and H. Hosono, *J. Am. Chem. Soc.* **130**, 3296 (2008).
- ⁸T. Kato, K. Yoshizawa, and K. Hirao, *J. Chem. Phys.* **116**, 3420 (2002).
- ⁹T. Kato, T. Kambe, and Y. Kubozono, *Phys. Rev. Lett.* **107**, 077001 (2011).
- ¹⁰A. Subedi and L. Boeri, *Phys. Rev. B* **84**, 020508(R) (2011).
- ¹¹M. Casula, M. Calandra, G. Profeta, and F. Mauri, *Phys. Rev. Lett.* **107**, 137006 (2011).
- ¹²G. Giovannetti and M. Capone, *Phys. Rev. B* **83**, 134508 (2011).
- ¹³G. H. Zhong, C. Zhang, G. F. Wu, Z. B. Huang, X. J. Chen, and H. Q. Lin, *J. Appl. Phys.* **113**, 17E131 (2013).
- ¹⁴T. Kosugi, T. Miyake, S. Ishibashi, R. Arita, and H. Aoki, *J. Phys. Soc. Jpn.* **78**, 113704 (2009).
- ¹⁵P. L. de Andres, A. Guijarro, and J. A. Verges, *Phys. Rev. B* **83**, 245113 (2011).
- ¹⁶T. Kosugi, T. Miyake, S. Ishibashi, R. Arita, and H. Aoki, *Phys. Rev. B* **84**, 214506 (2011).

- ¹⁷H. Okazaki, T. Wakita, T. Muro, Y. Kaji, X. Lee, H. Mitamura, N. Kawasaki, Y. Kubozono, Y. Yamanari, T. Kambe, T. Kato, M. Hirai, Y. Muraoka, and T. Yokoya, *Phys. Rev. B* **82**, 195114 (2010).
- ¹⁸Q. W. Huang, J. Zhang, A. Berlie, Z. X. Qin, X. M. Zhao, J. B. Zhang, L. Y. Tang, J. Liu, C. Zhang, G. H. Zhong, H. Q. Lin, and X. J. Chen, *J. Chem. Phys.* **139**, 104302 (2013).
- ¹⁹X. M. Zhao, J. Zhang, A. Berlie, Z. X. Qin, Q. W. Huang, J. Shan, J. B. Zhang, L. Y. Tang, J. Liu, C. Zhang, G. H. Zhong, H. Q. Lin, and X. J. Chen, *J. Chem. Phys.* **139**, 144308 (2013).
- ²⁰S. Fanetti, M. Citroni, L. Malavasi, G. A. Artioli, P. Postorino, and R. Bini, *J. Phys. Chem. C* **117**, 5343 (2013).
- ²¹F. Capitani, M. Höppner, B. Joseph, L. Malavasi, G. A. Artioli, L. Baldassarre, A. Perucchi, M. Piccinini, S. Lupi, P. Dore, L. Boeri, and P. Postorino, *Phys. Rev. B* **88**, 144303 (2013).
- ²²T. Pichler, M. Matus, J. Kurti, and H. Kuzmany, *Phys. Rev. B* **45**, 13841 (1992).
- ²³S. Fujiki, Y. Kubozono, S. Emura, Y. Takabayashi, S. Kashino, A. Fujiwara, K. Ishii, H. Suematsu, Y. Murakami, Y. Iwasa, T. Mitani, and H. Ogata, *Phys. Rev. B* **62**, 5366 (2000).
- ²⁴T. Kambe, X. He, Y. Takahashi, Y. Yamanari, K. Teranishi, H. Mitamura, S. Shibasaki, K. Tomita, R. Eguchi, H. Goto, Y. Takabayashi, T. Kato, A. Fujiwara, T. Kariyado, H. Aoki, and Y. Kubozono, *Phys. Rev. B* **86**, 214507 (2012).
- ²⁵A. Bree, F. G. Solven, and V. V. B. Vilkos, *J. Mol. Spectrosc.* **44**, 298 (1972).
- ²⁶P. C. Eklund, G. Dresselhaus, M. S. Dresselhaus, and J. E. Fischer, *Phys. Rev. B* **21**, 4705 (1980).
- ²⁷A. M. Rao, P. C. Eklund, S. Bandow, A. Thess, and R. E. Smalley, *Nature* **388**, 257 (1997).
- ²⁸G. Kresse and J. Furthmüller, *Comput. Mater. Sci.* **6**, 15 (1996).
- ²⁹J. P. Perdew and Y. Wang, *Phys. Rev. B* **45**, 13244 (1992).
- ³⁰A. Ruff, M. Sing, R. Claessen, H. Lee, M. Tomić, H. O. Jeschke, and R. Valentí, *Phys. Rev. Lett.* **110**, 216403 (2013).
- ³¹J. Heyd, G. E. Scuseria, and M. Ernzerhof, *J. Chem. Phys.* **118**, 8207 (2003).
- ³²J. Heyd and G. E. Scuseria, *J. Chem. Phys.* **121**, 1187 (2004).
- ³³J. Heyd, G. E. Scuseria, and M. Ernzerhof, *J. Chem. Phys.* **124**, 219906 (2006).